Numerical Tools for Slow Growth Approaches to Damage Tolerant Composite Aeronautical Structures

M. Khella[1], S. Ghiasvand[1], P. Ballarin[1], F. Panzeri[1], S. Piacquadio[1] & A. Airoldi[1]

[1]Dept. of Aerospace Science and Technology, Politecnico di Milano, Via La Masa 34, 20156, Milano, Italy – Ph. +39 02 2399 8363

Abstract

A contribution towards the pratical implementation of a Slow-Growth design approach for aeronautical composite structures is presented. Efforts towards the predictability of the residual strength in the presence of damage under static conditions are presented, and a first attempt at simulating the fatigue life of composite components with Finite Element (FE) models is illustrated. Results show a solid capability of current modelling approaches at predicting the response under quasi-static loads. Fatigue simulations of damage propagation in simple specimens give promising results, which encourage further efforts on this front.

Keywords: Damage Tolerance, Slow Growth, Fatigue growth prediction.

1. Introduction

A Damage Tolerant design and operation of composite structures requires an accurate knowledge of the evolution of damage under service loads. To be accepted on commercial structures, damage growth must be proven to be slow, stable, and predictable, to the satisfaction of Regulatory Authorities (AMC 20-29 (EASA) [1]—AC 20-107B (FAA) [2]). Numerical models for the prediction of residual static strength of composite structures are widespread and mature in the literature [3]. On the other hand, an accurate, reliable and, at the same time, efficient and scalable [4], tool for the simulation of damage growth under cyclic loads has not yet come to the same maturity.

For this and other reasons — e.g., difficulty in assessing damage evolution with state-of-the-art inspection techniques [5] — the No-Growth approach [1, 2] to composite design has always been the standard on commercial aircraft structures, a design philosophy whereby damage is not allowed to grow under cyclic loads. This is achieved by oversizing structural members to maintain stresses very low, which comes at a severe weight penalty, which could be avoided if reliable predictive tools were available. Among the many different damage modes, delamination damage occurs most easily (even by low-velocity impacts), it can severely undermine structural integrity, and is nearly undetectable [6]. Therefore, we have decided to focus our efforts on the prediction of delamination growth.

The efforts presented here are an advancement towards the implementation of the Slow-Growth approach for the design of aeronautical structures. We pursue this end-goal by assessing the developed numerical tools to predict the response of composite laminates. Two are the fundamental aspects for the development of a numerical approach to accomplish such objective:

1. the prediction of residual strength of structural elements in the presence of damage (and of delamination in particular);

2. the prediction of delamination propagation under fatigue loading.

2. Damage Tolerance under Static Loading

2.1 Experimental Tests

Damage tolerance under static loading was studied on L-shaped UD carbon fibre specimen (representative of a helicopter blade root component). Specimens were manufactured with a $[0]_{48}$ lay-up. A pre-damage, produced by using a double folded Teflon sheet that was positioned in the curved part between two adjacent layers. Different pre-crack lengths of 2, 3, 4, and 5 mm were adopted. Pre-cracks were all positioned at 1/3 of the thickness from the internal side of the specimens. Tests were performed applying a traction to end of the legs of the L-shaped specimens. The pictures reported in 1-(A) and 1-(B) show the initial damage of two specimens and the post-failure configurations, which was characterized by a crack propagating from the initial damage and a final crack occurred above the position of the pre-cracks.

The experimental evidence, summarized in Fig. 1, demonstrates that all the specimens showed the same failure pattern. Initially, the pre-crack started propagating when a certain level of load is reached, then, by continuing the application of the load, the crack propagated up to the half of the specimens legs. Finally, catastrophic failure occurred in the upper curved region (the two-thirds of thickness above the pre-cracked interface), which can be observed in Fig. 1.

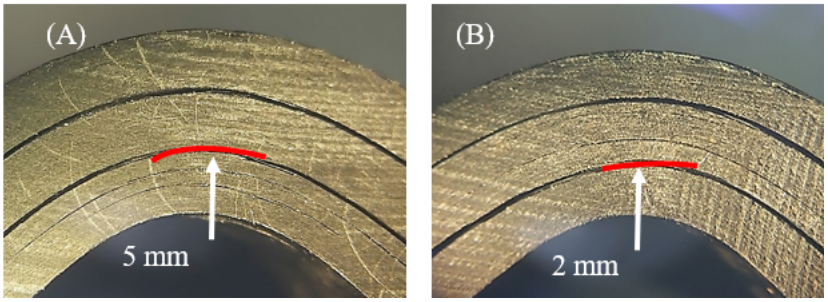

Figure 1 – Initial pre-crack and post-failure configuration of L-shaped specimens with a defect of 5 mm (A) and a defect of 2 mm (B).

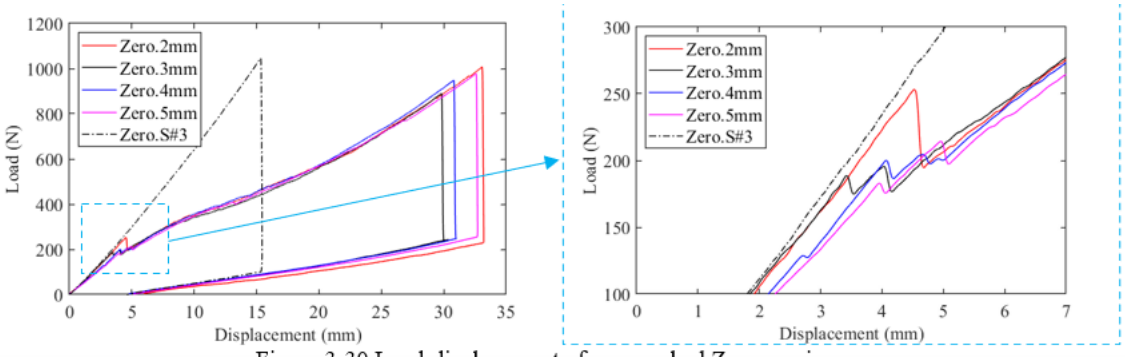

Figure 2 – Force vs. displacement curves obtained in opening tests of L-Shaped specimens with and without pre-cracks.

The force-displacement response of the pre-cracked specimens is compared to that of a pristine one in Fig. 2. The presence of the pre-crack produces a relevant reduction in the load necessary for crack propagation (from 1100 N for the pristine specimen to 200-250 N for the pre-cracked specimens), obtaining a stable damage propagation much more "gentle", and less catastrophic compared to that observed in the specimens in pristine conditions. What we can also observe is that the load necessary for damage propagation was nearly independent of the size of damage (Fig. 3-(C)).

2.2 Static Test Simulations

The bi-phasic modelling technique presented in [7] and applied to predict the strength of different types of composites in [8, 9] was the one used for the simulation of the pre-cracked L-shaped specimens. The approach is based on a bi-phasic decomposition of the composite properties, whereby a

cohesive zone model is embedded in solid elements, that can reproduce both in-plane matrix cracking and delamination in a very easy and seamless fashion [7, 8, 9]. The results produced by the simulation, reported in Fig. 3, show that the approach can yield very accurate predictions for the onset of damage propagation under static loading (Fig. 3-(A)), the final failure mode (Fig. 3-(B)), and the residual-strength vs damage size curve (Fig. 3-(C)). These results confirm the reliability of the method for the prediction of the static response of a pre-damaged element.

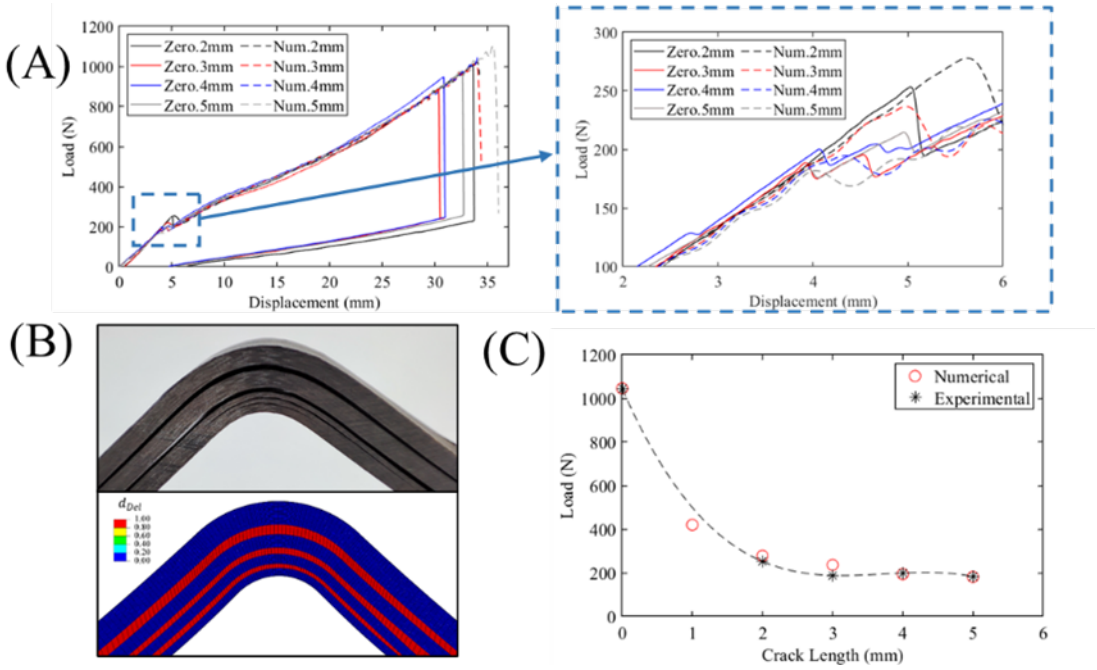

Figure 3 – Numerical-experimental correlation obtained in the simulation of pre-cracked specimens: (A) force vs. displacement curves, (B) failure mode, and (C) residual strength vs. initial damage size.

3. Predictability of Damage Tolerance under Fatigue Loading

3.1 Fatigue Simulation Framework

Whereas the FE simulation of a quasi-static test in its entirety is possible, a cycle-by-cycle fatigue simulation would be impractical because of the computational cost it would entail. In our work, we have employed the Simplified-Cyclic Loading (SCL) technique to simulate fatigue damage, which relies on a number of simplifying assumptions, which have to do with the structure and the loads it is subjected to. These assumptions are, in essence:

1. Absence of non-linearities, such as geometrical and material non-linearities, residual thermal stresses, etc.

2. Synchronous loads and, in general, loads that do not involve a variation in load direction during a cycle

3. Constant-amplitude load spectra, where the minimum and maximum load/displacements are unique throughout the whole load spectrum

The foregoing assumptions may be done away with, but at the cost of more sophisticated simulation strategies, such as the Min-Max and the Cycle-Jump techniques [10]. If, however, they are not overly restrictive for our interests, we may use the SCL simulation scheme.
An SCL fatigue simulation consists of a first step in which load is introduced in the structure quasi-statically, until the upper bound of the load-block to be simulated (max-load), at which point is held constant. Fatigue damage is introduced through a properly-formulated and calibrated fatigue damage accumulation law. In Fig. 4 the cyclic oscillation shown in the graph is not the load that is really

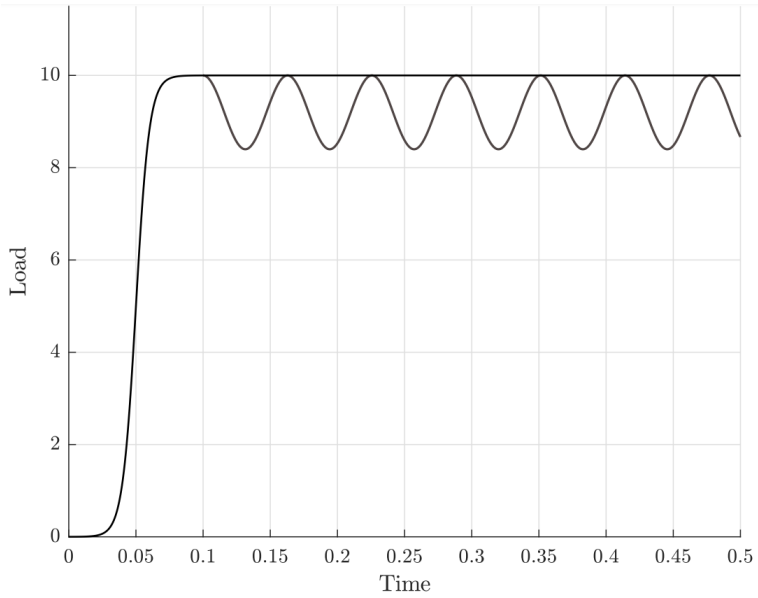

Figure 4 – Example of an SCL load

applied, but its effect is accounted for by means of the damage accumulation law, while the constant leg is what is actually simulated.
The damage accumulation law is a function of the form of Eq. 1

$$\frac{dD}{dN} = f\left(D, R, \frac{\sigma_{max}}{\sigma_c}\right) \tag{1}$$

That is, fatigue damage depends on the state of damage itself, D, the stress ratio R (which accounts for load cycling, since cycling is not actually simulated) and the stress severity level, σ_{max}/σ_c, the ratio of element stress to material strength. Considering the actual finite element simulation, a finite amount of load cycles is applied at each time increment, so that the state of damage following the application of said load cycles (Eq 2) is calculated and applied to the structure, which is applied to the model at the next time step.

$$D_{k+1} = D_k + f\left(D_k, R, \frac{\sigma_{max,k}}{\sigma_c}\right)\Delta N_k \tag{2}$$

The results presented in this paper were obtained from explicit simulations, so that the finite-difference increment estimated by Eq. 2 is a reasonable estimate for the D_{k+1} state of damage.

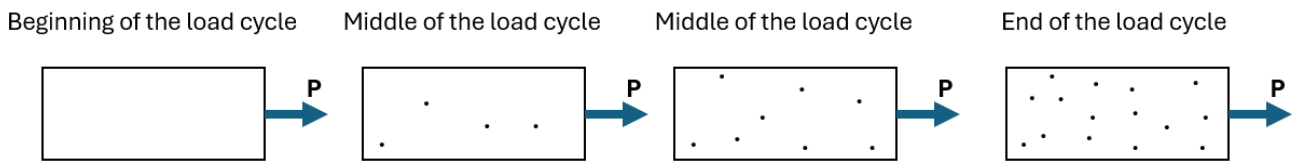

Figure 5 – Accumulation of damage (the dots) within one loading cycle.

To provide further clarity on why the maximum load is held constant, and why it may be considered a reasonable assumption to simulate for fatigue damage in this way, let us consider the following. For a given structure under a load cycle (load-unload), we may imagine the formation of fatigue damage inside the structure to be distributed throughout the load cycle itself (see Figure 5; in the figure, damage is represented by the dots, which increase as the load increases within a fatigue cycle). In other terms, as soon as we start to load the structure, damage begins to form; then, more damage is produced as we increase loads, until we reach the maximum load of that given load cycle.

A first, fundamental, simplification is that of concentrating a whole cycle's damage in the instant of highest loading. In this way, no damage is accrued to the structure throughout the loading history until the maximum load is reached: at this point damage is accrued all at once, as Fig. 6 illustrates. SCL removes the need for a cycle-by-cycle simulation of the fatigue event by means of this assumption, which concentrates damage introduction in the instant of max-loading, eliminating the need of simulating the entire loading history. If damage is what we are after, and damage is concentrated at the maximum-load instant, then we need only simulate the point of maximum-load, and increment damage by maintaining it.

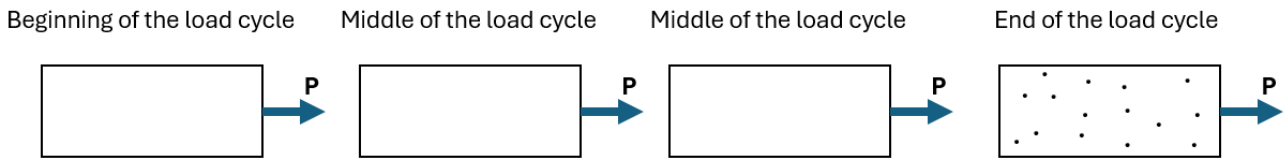

Figure 6 – SCL idealization for the damage-introduction process within a load-cycle.

3.2 Validation on Fundamental Specimens: DCB and ENF

However accurate and reliable the static modeling of damage tolerance may be, it alone would not suffice for an efficient and rationalized deployment of a Slow Growth approach to the structural design of composites, unless the tool be endowed with the capability of predicting the onset of crack growth and the evolution of its propagation under cycling loading, that is under the action of fatigue operational loads. Simplified, empirically calibrated models for the prediction of delamination growth under cycling loading have recently been proposed in the literature [11, 12]. The numerical approach adopted for delamination modelling is based on a Cohesive Zone Model, where the accumulation of fatigue damage is simulated with the SCL technique.

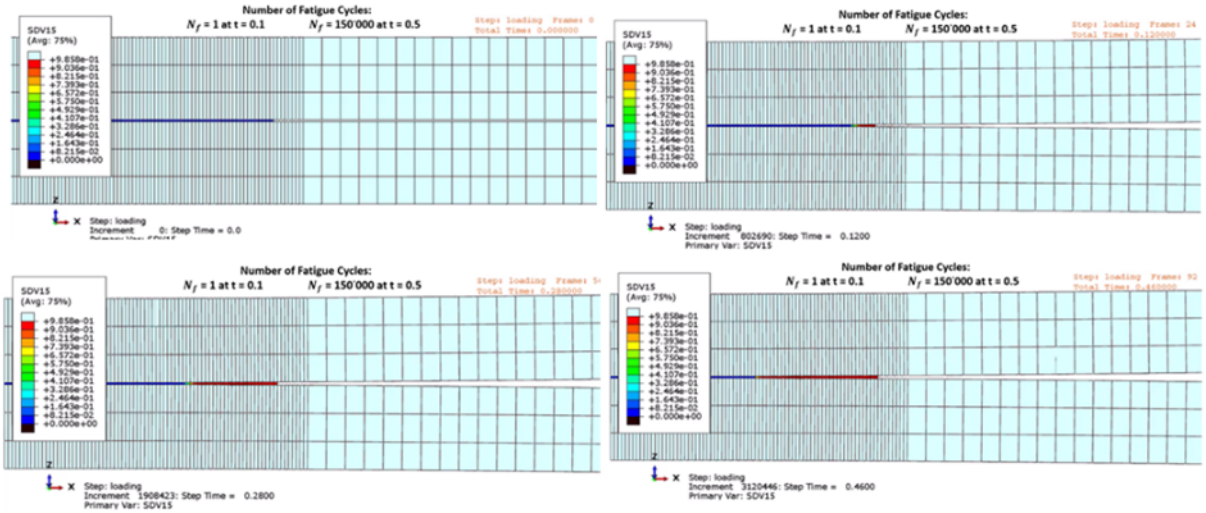

Figure 7 – Sequence taken from the simulation of crack propagation in a Double Cantilever Beam specimen.

One of the most promising model, presented in [12], has been implemented within the cohesive modelling approach developed and assessed in [7, 8, 9]. The sequence reported in Fig. 7 is referred to the simulation of the Mode I opening of a Double Cantilever Beam (DCB) specimen. The numerical activity has been also extended to Mode II opening by simulating an End Notched Flexure specimen (ENF). The analyses allowed us to obtain the crack growth rates for different values of opening displacements, as reported in Fig. 8 and 9. These figures report the comparison between the

numerical crack growth rate obtained by the model developed in this activity, represented by the discrete symbols, and the experimental results presented in [11, 13].

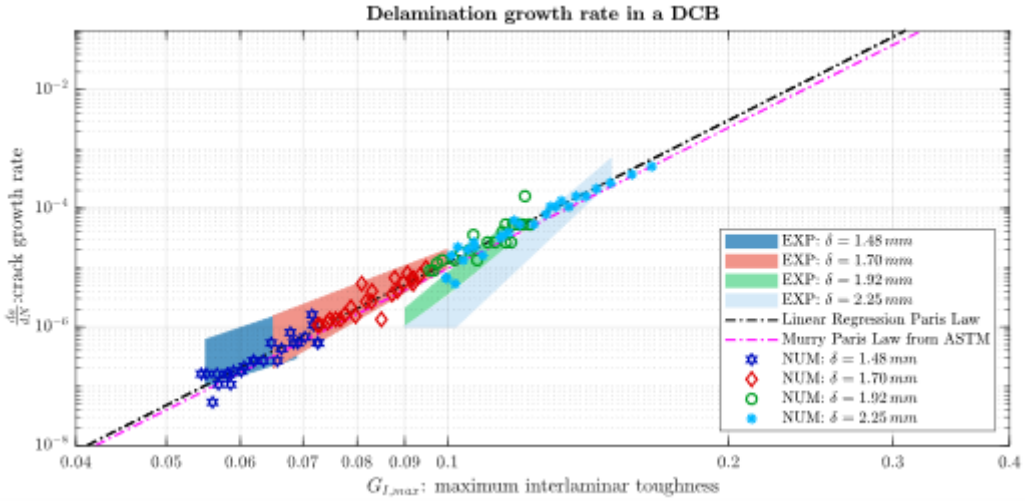

Figure 8 – Numerical-experimental correlation obtained in the simulation performed for a DCB coupons.

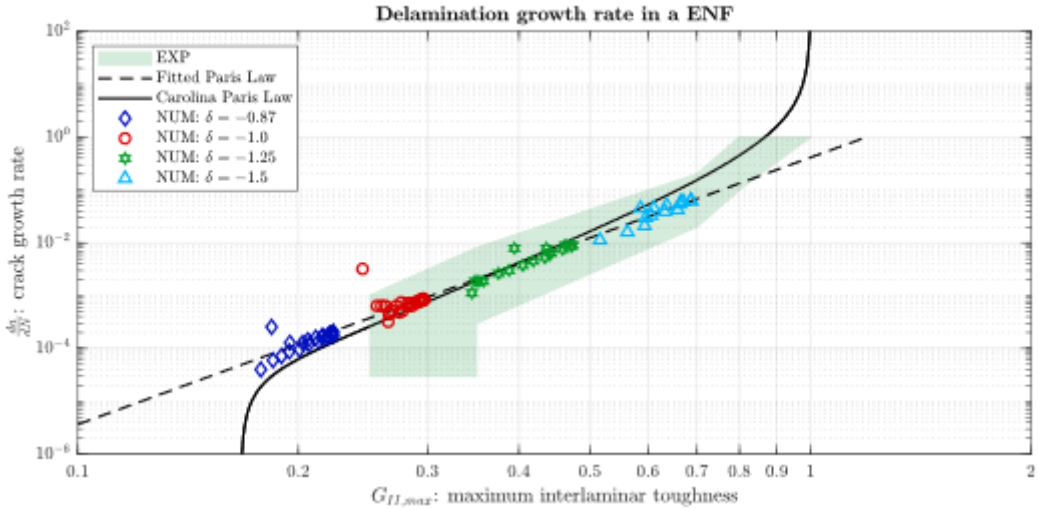

Figure 9 – Numerical-experimental correlation obtained in the simulation performed for a ENF coupons.

The results of the models for the quasi-static simulation of crack propagation (Fig. 3), and those of the fatigue modelling approach (presented in figures 8 and 9) encourage more efforts towards the assessment of the modelling strategy. In the next subsection we will present the assessment of a numerical model for the simulation of the crack-growth of a pre-delaminated L-shaped specimen under fatigue loading.

3.3 Assessment of the Numerical Model of the L-shaped Specimen under Fatigue Loading

Having validated and calibrated our fatigue damage model on DCB and ENF specimens, we constructed a 1/10-wide slice model of the pre-damaged L-shaped specimen (Fig. 10) and simulated its fatigue behaviour.

The model is intended for a preliminary evaluation of the capabilities of the modelling framework presented previously in reproducing the fatigue behaviour of the L-shaped specimen studied during the previous activity. Therefore, the simplest solution for its modelling was thought implemented. Only one line of cohesive elements was included in the whole model, inserted in the pre-damaged interface

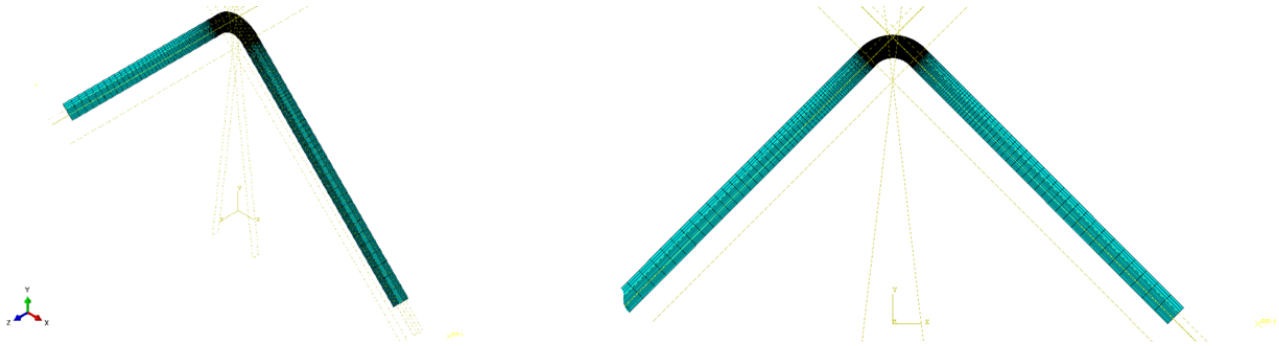

Figure 10 – Finite element model for the L-shaped specimen.

(Fig. 11), as damage is expected to start and propagate at that one first (as is also evidenced by static tests on the same specimen). The rest of the composite laminate was modelled with continuum shell elements.

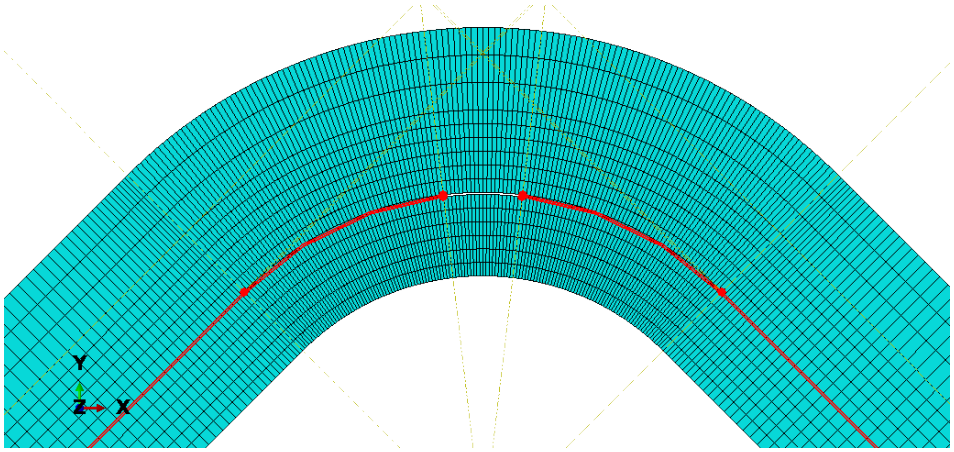

Figure 11 – Close up view of the L-shaped specimen (in red is highlighted the (only) cohesive interfaced modelled).

Going on to the results of the model, we have characterized its behavior for two different pre-crack lengths: $a_0 = 2$ mm and $a_0 = 4$ mm. A constant loading block was applied, to represent the cycling of the specimen between a maximum and a minimum displacement (δ_{max} and δ_{min}). The ratio between these two quantities, also known as stress ratio R, was set = 0.1. In Fig. 12 the crack length is presented as a function of cycles applied on the $a_0 = 2$ mm model, for three different maximum applied displacements, δ_{max} (simply "delta", in the figure legend). As can be seen, growth is prevented under about 250'000 cycles for the delta = 2.00 mm case, under about 150'000 cycles for the delta = 2.10 mm case, and under about 95'000 cycles for the delta = 2.20 mm case. On the other hand, after the intermediate sudden propagation, Δa reaches a 5mm length (the 5mm threshold was arbitrarily chosen) at about 450'000 cycles for the delta = 2.00 mm case, about 350'000 cycles for delta = 2.10 mm, and about 200'000 cycles for the delta = 2.20 mm case. Going down in maximum applied displacement, we may look for the δ_{max} value for which no propagation occurs for at least 1 million cycles. This happens at delta = 1.70 mm, for which no propagation is seen under about 1.3 million cycles.

The same simulations were run on the $a_0 = 4$ mm model, to which the same, constant loading block was applied, with R =0.1, and at different δ_{max} values. In Fig. 13 we see the crack length vs. the cycles applied, at δ_{max} = 1.90 mm, 2.00 mm and 2.10 mm. What we see in this case is that crack growth starts much earlier: at about 13'000 cycles for the delta = 1.90 mm case, about 5'000 cycles for the delta = 2.00 mm case, and about 3'000 cycles for the delta = 2.10 mm case. The crack reaches the Δa =4 mm threshold at 400'000 cycles in the delta = 1.90 mm case, at 125'000 cycles in the delta = 2.00 mm case, at 95'000 cycles in the delta = 2.10 mm case. At δ_{max} = 1.70 mm, no propagation is seen under 1 million cycles.

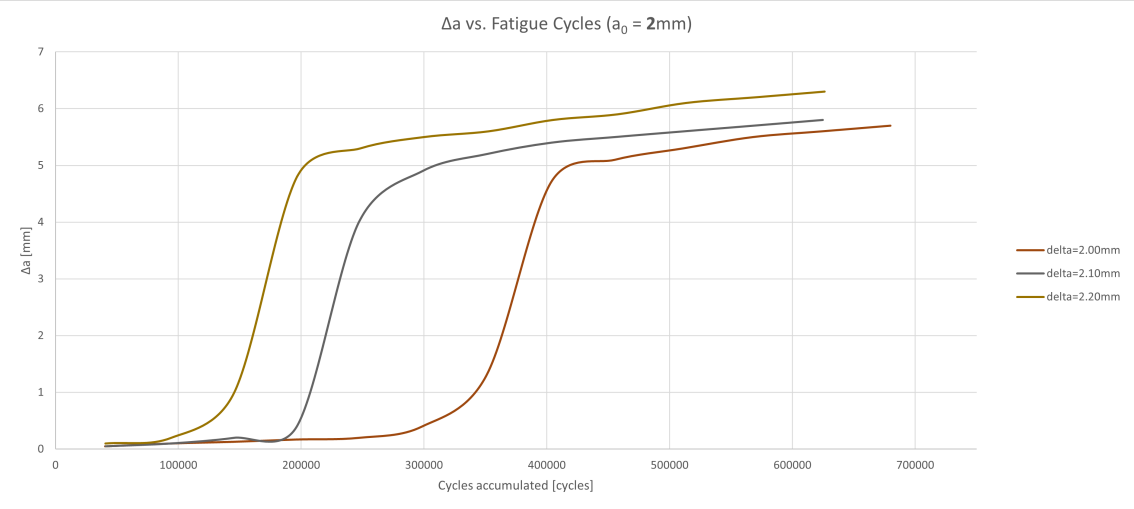

Figure 12 – Crack length increment vs. Load cycles applied, on the model with a 2mm pre-crack.

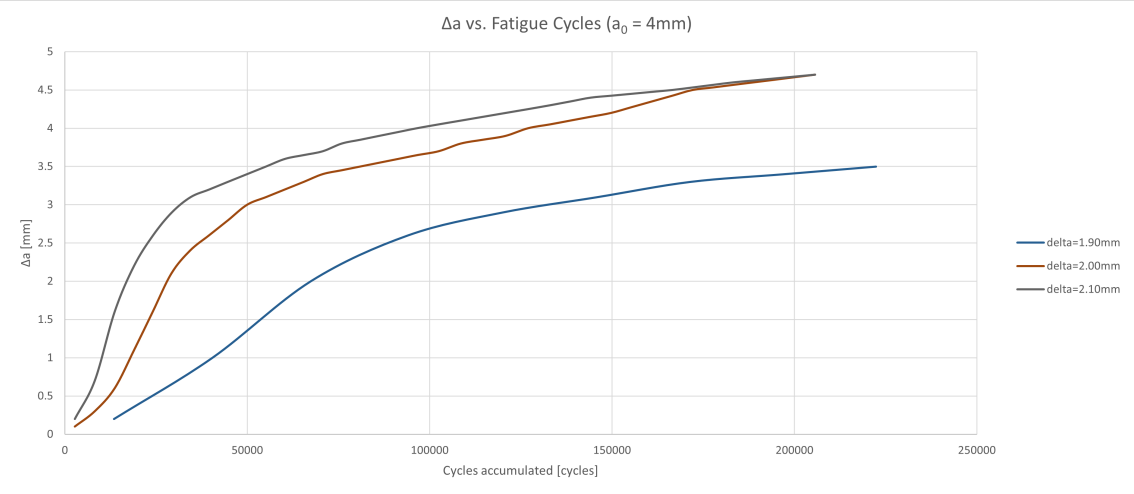

Figure 13 – Crack length increment vs. Load cycles applied, on the model with a 4mm pre-crack.

In the following figures, we report the crack growth at different instants of the cycling process, once from the front, in Fig. 14, and then in a perspective view, in Fig. 15.
Colored red are the elements whose fatigue resistance has been wholly consumed. Therefore, the sequence of images proposed in figures 14 and 15 show the advancement of the delamination front, as cycles are being applied to the structure.
The results predicted a reasonable response of the specimen, although they still need to be accurately and quantitatively evaluated through an experimental campaign.

4. Summary and Concluding Remarks

A Slow-Growth approach to composites design and certification for aeronautical structures requires demonstrating that the growth of damage be slow, stable and predictable. The task of designing a structure that undergoes slow and stable damage growth is not trivial and could require several design iterations. The approach hereby presented promises to predict delamination growth and reduce the experimental effort required for designing Slow-Growth composite structures. The biphasic modelling approach presented and assessed in [7, 8, 9] proves to be both computationally efficient, and doesn't determine any loss of accuracy compared to the more conventional and widely adopted approaches for composites modelling. It capabilities were assessed on static tests on an L-shaped composite laminate, proving the foregoing statements. A recently proposed FE framework for fatigue modelling [11] was implemented within this modelling approach, and assessed against DCB and ENF fatigue tests from the literature, providing encouraging results about its potentialities for more complex appli-

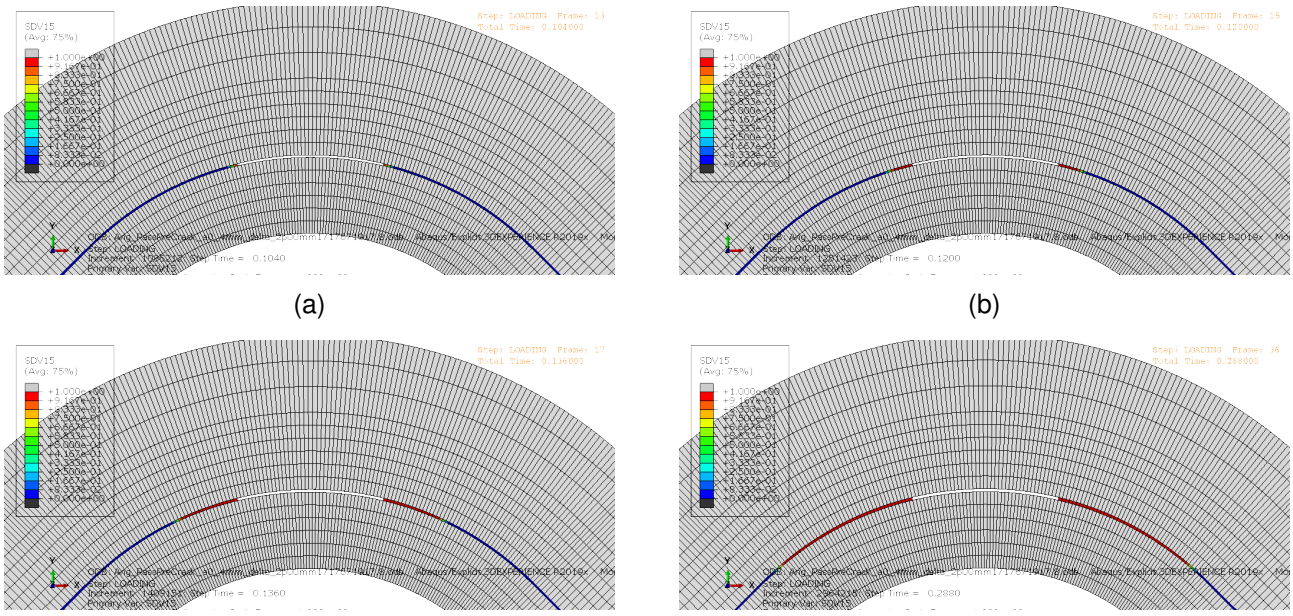

(a) (b) (c) (d)

Figure 14 – Sequence taken from the simulation of crack propagation of a pre-cracked L-shaped specimen (front view). Sequence taken at: (a) 3'000 cycles; (b) 13'000 cycles; (c) 30'000 cycles; (d) 90'000 cycles.

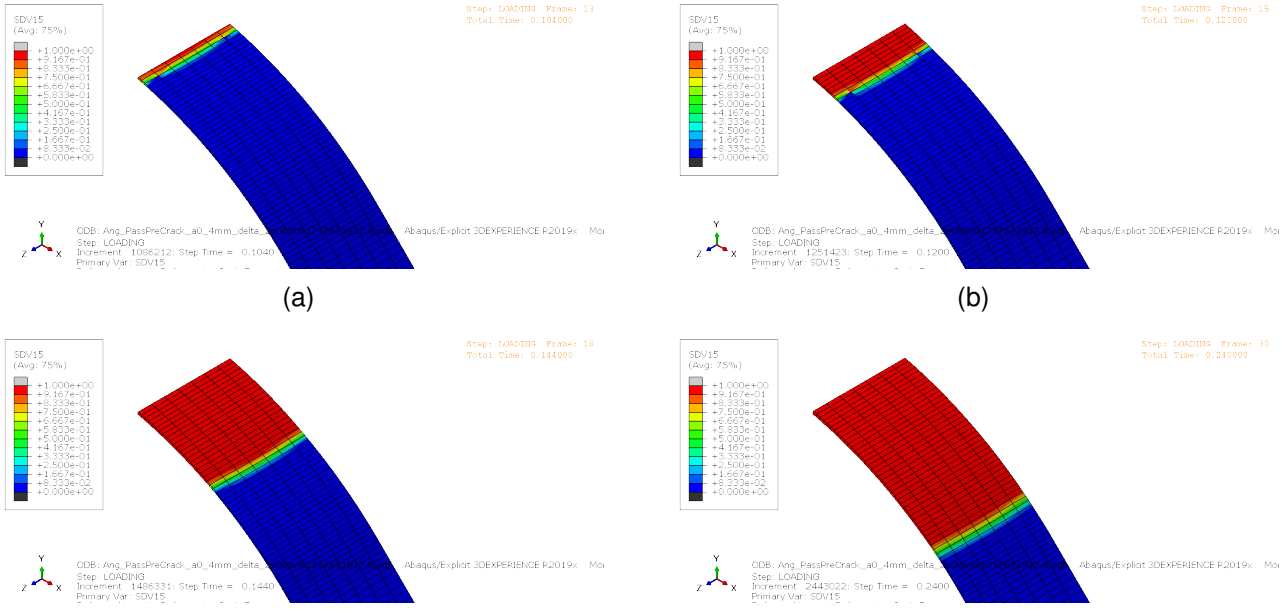

(a) (b) (c) (d)

Figure 15 – Sequence taken from the simulation of crack propagation of a pre-cracked L-shaped specimen (perspective view; only the interface elements are shown). Sequence taken at: (a) 3'000 cycles; (b) 13'000 cycles; (c) 30'000 cycles; (d) 90'000 cycles.

cations. Therefore, a model of the L-shaped specimen was built and characterized, producing results that, for the present moment, prove themselves to be reasonable. Further experimental activity is in program to conduct fatigue tests on this very specimen, which would provide the data needed to validate, or better calibrate, our current fatigue model.

5. Contact Author Email Address

Corresponding author: maikel.khella@polimi.it

6. Copyright Issues

References

[1] AMC 20-29, 'Certification Specifications (CSs)', EASA.

[2] 'AC 20-107B - Composite Aircraft Structure', FAA.

[3] Liu, P. (2021) *Damage Modeling of Composite Structures: Strength, Fracture, and Finite Element Analysis*. *Elsevier*.

[4] Leone, F. A., Davila, C. G. (2021). *Scalability of Cohesive Fatigue Analyses Using Explicit Solvers*. In *AIAA Scitech 2021 Forum* (p. 0314).

[5] Pascoe, John-Alan. *Slow-growth damage tolerance for fatigue after impact in FRP composites: Why current research won't get us there. Theoretical and Applied Fracture Mechanics* 116 (2021): 103127.

[6] Reid, Stephen Robert, and Gang Zhou, eds. Impact behaviour of fibre-reinforced composite materials and structures. Elsevier, 2000.

[7] Airoldi, A., Mirani, C., Principito, L. (2020). *A bi-phasic modelling approach for interlaminar and intralaminar damage in the matrix of composite laminates*. *Composite Structures*, 234, 111747.

[8] Airoldi, A., Novembre, E., Mirani, C., Gianotti, G., Passoni, R., Cantoni, C. (2023). A model for damage and failure of carbon-carbon composites: development and identification through Gaussian process regression. Materials Today Communications, 35, 106059.

[9] Ghiasvand, S., Airoldi, A., Sala, G., Aceti, P., Ballarin, P., Baldi, A., Mesiani, E. (2023). Meso-Scale Models to Analyse the Interactions of Damage Modes in Composites Laminates. In 31st ICAF Symposium (pp. 1-15).

[10] Raimondo, A., Bisagni, C. (2020). *Analysis of local stress ratio for delamination in composites under fatigue loads*. *AIAA Journal*, 58(1), 455-463.

[11] Dávila, C. G. (2020). *From SN to the Paris law with a new mixed-mode cohesive fatigue model for delamination in composites*. *Theoretical and Applied Fracture Mechanics*, 106, 102499.

[12] Dávila, C. G., Rose, C. A., Murri, G. B., Jackson, W. C., Johnston, W. M. (2020). *Evaluation of fatigue damage accumulation functions for delamination initiation and propagation* (No. NF1676L-36100).

[13] Panduranga, R., Shivakumar, K. (2017). Mode-II total fatigue life model for unidirectional IM7/8552 carbon/epoxy composite laminate. International Journal of Fatigue, 94, 97-109.